Published in final edited form as:
J Magn Reson Imaging. 2010 January ; 31(1): 255–261. doi:10.1002/jmri.22019.

Dual-Echo Arteriovenography Imaging with 7 Tesla MR

Kyongtae Ty Bae, MD, PhD[1], **Sung-Hong Park, PhD**[2], **Chan-Hong Moon, PhD**[1], **Jung-Hwan Kim, MS**[1], **Diana Kaya, MD**[1], and **Tiejun Zhao, PhD**[3]

[1]Department of Radiology, University of Pittsburgh, Pittsburgh, PA

[2]Research Imaging Center, University of Texas Health Science Center at San Antonio, TX

[3]MR R&D, Siemens Healthcare, Pittsburgh, PA

Abstract

Purpose—To implement a dual-echo sequence MR imaging technique at 7T for simultaneous acquisition of time-of-flight (TOF) MR angiogram (MRA) and blood oxygenation level-dependent (BOLD) MR venogram (MRV) in a single MR acquisition and to compare the image qualities with those acquired at 3T.

Materials and Methods—We implemented a dual-echo sequence with an echo-specific K-space reordering scheme to uncouple the scan parameter requirements for MRA and MRV at 7T. The MRA and MRV vascular contrast was enhanced by maximally separating the K-space center regions acquired for the MRA and MRV and by adjusting and applying scan parameters compatible between the MRA and MRV. The same imaging sequence was implemented at 3T. Four normal subjects were imaged at both 3T and 7T. MRA and MRV at 7T were reconstructed both with and without phase-mask filtering and were compared with those at 3T with phase-mask filtering quantitatively and qualitatively.

Results—The depiction of small cortical arteries and veins on MRA and MRV at 7T was substantially better than that at 3T, due to about twice higher contrast-to-noise ratio for both arteries (164±57 vs. 77±26) and veins (72±8 vs. 36±6). Even without use of the phase-masking filtering, the venous contrast at 7T (65±7) was higher than that with the filtering at 3T (36±6).

Conclusion—The dual-echo arteriovenography technique we implemented at 7T allows the improved visualization of small vessels in both the MRA and MRV because of the greatly increased SNR and susceptibility contrast, compared to 3T.

Keywords

High-field MR; MR angiography; time-of-flight; blood-oxygenation-level-dependent venography; susceptibility-weighted imaging; brain imaging; dual-echo technique; CODEA

Introduction

As the magnetic field strength increases, both the signal-to-noise ratio (SNR) and the spectral resolution of the MR signal increase (1). Potential advantages of clinical imaging at high-field MR include higher spatial resolution, enhanced tissue contrast, shortened acquisition time and more sensitive functional MRI and MR spectroscopy. High resolution allows us to image smaller structures with greater and more accurate anatomical definition. Increased magnetic susceptibility at high fields enhances T2*-based MR venous contrast

*Correspondence to: Kyongtae Ty Bae, MD, PhD, Department of Radiology, School of Medicine, University of Pittsburgh, FARP/Imaging Research, 3362 Fifth Ave., Pittsburgh, PA 15213, Telephone: 412-641-2657, Fax: 412-641-2582, baek@upmc.edu.

(2,3). For instance, ultra-high-field (UHF) MR imaging such as 7T imaging has recently shown markedly enhanced SNR, blood-to-tissue contrast, and susceptibility effect that improve the visualization of small arteries and veins in the brain (4,5).

Time-of-flight (TOF) MR angiography (6) is routinely used in clinical brain imaging studies, providing information of detailed arterial vasculature. As a complementary vascular imaging modality, blood oxygenation level-dependent (BOLD) MR venography (2,3) has been performed and used for delineation of venous anatomy in the brain (7–10). In clinical brain imaging studies, imaging both TOF MR angiogram (MRA) and BOLD MR venogram (MRV) are often desirable, because they complement the depiction of vascular pathologies. Nevertheless, MRV is not routinely acquired to minimize the image acquisition time.

Recent studies have reported new technical developments relating to the simultaneous acquisition of both TOF MRA and BOLD MRV using the scan time required for only one, MRA or MRV (11–13). In particular, Park et al. (13) developed and demonstrated a compatible dual-echo arteriovenography (CODEA) technique in which dual-echo scan parameters (compatible for both the MRA and MRV vascular contrast) were achieved by exploring K-space characteristics and employing an echo-specific K-space reordering scheme. The CODEA technique permitted the acquisition of a simultaneous dual-echo MRA and MRV that achieved image quality comparable to that of the conventional single-echo MRA and MRV, separately acquired at two different sessions. Furthermore, some MR angiographic techniques commonly used in conventional 3D TOF MRA such as multiple overlapping thin-slab acquisition (MOTSA) (14) and magnetization transfer contrast (MTC) pulse (15,16), are effectively applicable to the CODEA technique (13). When taking advantage of both the CODEA technique and ultra-high-field MR acquired at 7T, we would attain improved visualization of small vessels in MRA and MRV due to greatly increased SNR and susceptibility contrast. The enhanced susceptibility contrast at 7T may even remove the requirement of phase-mask filtering in venogram (17). Although phase-mask filtering is useful for increasing the visibility of the venous vasculature in MRV, particularly at low-fields (18), it is time consuming and often introduces unwanted susceptibility artifacts. MRV at 7T without phase-mask filtering makes the venographic imaging technically more straightforward and reliable. Thus, the purpose of this study was to implement a dual-echo sequence MR imaging technique at 7T for simultaneous acquisition of TOF MRA and BOLD MRV in a single MR acquisition and compare the image qualities with those acquired at 3T.

Materials and Methods

Institutional review board approval was obtained for this HIPAA-compliant study and informed consent was obtained from each patient.

Compatible Dual-echo Arteriovenography (CODEA) Technique

The CODEA technique introduced and tested in a recent study at 3T (13) was implemented at 7T following the same principle. Briefly, the K-space center region of MRA (first echo) and the edge region of MRV (second echo) are acquired during the first half, and the K-space edge region of MRA and center region of MRV during the second half of the complete data acquisition, as described in Fig. 1. The 1st PE in the figure corresponds to the in-plane phase encoding direction while the 2nd PE to the slice encoding direction. This K-space data acquisition scheme allows for the maximum separation between the two K-space center regions along the 1st PE direction, which typically has higher spatial resolution than the 2nd PE direction. To enhance vascular-specific tissue contrast, RF pulse parameters advantageous for MRA (ramped excitation RF pulse with a higher flip angle) are applied during the first half (K-space center region of MRA) while those advantageous for MRV

(flat excitation RF pulse with a lower flip angle) are applied during the second half (K-space center region of MRV). In our implementation, the 1st PE loop was located outside the 2nd PE loop; the K-space was filled along the 2nd PE direction at the initial 1st PE location and repeated at subsequent1st PE locations until the 1st PE loop was completed. Having only one transition in the RF pulse parameters between the two halves of the complete data acquisition helps minimize any potential perturbations in the steady-state condition.

CODEA Imaging at 7T and 3T

All experiments were performed on a 7T and a 3T whole-body human scanner (Siemens Medical Solutions, Erlangen, Germany). A vendor-provided 8-channel head coil was used for both transmission and reception at 7T, and a body coil and a 12-element head matrix coil were used for transmission and reception, respectively, at 3T. However, the 3T head matrix coil was set to the 8-channel dual mode. As a result, the number of channels used to receive the imaging data was the same for both 3T and 7T acquisitions. Four normal male volunteers were then scanned. At both 7T and 3T, a single-slab, dual-echo arteriovenogram was acquired with a 3D gradient echo sequence. First-order flow compensation was applied to both the slab-select and readout gradients (16,19). Imaging parameters were: TR = 35 ms, TE = 3.3 ms (1st echo)/20 ms (2nd echo), acquisition BW = 150 Hz/pixel (1st echo)/ 50 Hz/pixel (2nd echo), matrix size = 512×192×64, corresponding FOV = 240×180×80 mm^3, number of averages = 1, slice oversampling = 30%, and total scan time = 9.3 min. Partial (67%) and full echo samplings were used in the first and the second echoes, respectively. The K-space center region in the first echo (TOF-weighted region) was acquired with a minimum-phase ramped excitation pulse with flip angle of 25° (20°–30°), and the K-space center region in the second echo (BOLD-weighted region) with a minimum-phase flat-profile RF excitation with flip angle of 15°. In order to keep the specific absorption rate (SAR) low, neither spatial pre-saturation pulse nor MTC pulse was used.

For the 7T, an additional 3D CODEA dataset was acquired with higher spatial resolution of matrix size = 640×240×80, TR = 35 ms, TE = 3.6 / 21 ms, and total scan time = 14.5 min. The other scan parameters for this acquisition were the same as the aforementioned acquisition.

Image Reconstruction, Display, and Data Analysis

The three dimensional raw dataset from each RF channel was Fourier-transformed to 3D images with the matrix size of 512×384×170 for the lower resolution and 640×480×213 for the higher resolution using zero filling. Venous contrast of the MRV at 3T was enhanced using phase-mask filtering (20), while the MRV at 7T was reconstructed with and without the phase-mask filtering. Subsequently, 3D images from all the 8 channels were combined and averaged in magnitude mode to generate a single 3D dataset for 3T and 7T. These procedures were repeated for each echo to reconstruct MRA and MRV separately. MRA images were displayed in maximum-intensity projections over the entire volume, whereas MRV images in minimum-intensity projections over 10-mm thickness. For each subject, the MRA/MRV images acquired at 7T and 3T were displayed side-by-side and compared. In particular, the vascular signal conspicuity, depiction of vessels (including the small cortical arteries and veins), and the presence of artifact were evaluated qualitatively. The contrast to noise ratio (CNR) of the MRA and MRV blood vessels at 7T and 3T was computed and compared. This was achieved by measuring the signal intensities over a vascular region, a tissue region devoid of detectable blood vessels, and a background region outside the brain from the 3D images with no projection. A vascular region of interest (ROI) was determined first from the dataset of a subject at 3T and then assigned to the corresponding dataset at 7T for the same subject at the same anatomical location. The ROI selections were repeated for the other subjects for both 3T and 7T. The vascular ROI was selected large enough to

include the whole cross section and then averaged over a certain number of pixel signals of the highest intensities for arteries in MRA and again for those of the lowest intensities for veins in MRV. The number of pixels for the average was 20 (large), 10 (medium), and 5 (small) for arteries; and 15 (large), 10 (medium), and 7 (small) for veins. The measurement processes were repeated in the right and left hemispheres and averaged for each vascular ROI in each subject.

Results

CODEA MRA at 7T demonstrated significantly improved visualization of the small cortical arteries as compared to those scanned at 3T (Fig. 2). CODEA MRV at 7T also depicted far more detailed small cortical veins and venules in the cerebral cortex than at 3T (Fig. 3). We used a TE of 20 ms for CODEA MRV at 7T which was longer than the optimal TE previously reported for phase-mask filtering (~15 ms at 7T (5,21)). Even without a phase-mask filtering at the longer TE value, small veins were depicted in detail (Fig. 3d–f). The venous contrast was further enhanced by phase-mask filtering of CODEA MRV at 7T with the longer TE (Fig. 3g–i). The effect of the longer TE was evident with increased susceptibility artifact (Fig. 3g). These observations were consistent for all subjects

While the background signal intensity throughout the brain was relatively homogenous at 3T, we observed the signal intensity of the periphery of the brain to be higher than the center at 7T (Figs. 2 and 3). This is presumably due to differences in excitation RF coils between 3T and 7T. However, the relative inhomogeneity at 7T did not appear to compromise the delineation of small cortical arteries and veins.

CNR values of a few arteries and veins (Fig. 4) averaged over all volunteers are shown in Table 1. These vessels were mostly selected in the middle of the brain to minimize over estimation of CNR for 7T. Overall arterial CNR of the 7T CODEA MRA (164±57) was much higher than that of the 3T CODEA MRA (77±26). In addition, the overall venous CNR of the 7T CODEA MRV with and without phase-mask filtering (72±8 and 65±7) was higher than that of the 3T CODEA MRV with phase mask-filtering (36±6). Venous CNR values had much less deviation than the arterial CNR (Table 1), due to hypointense vascular contrast. The smallest arteries and veins both showed more significant increase in percent CNR values as compared to those of “medium” and “large” (Table 1). Venous CNR values in 7T CODEA MRV were improved overall by ~10% with the use of the phase-mask filtering (Table 1). Owing to the increased CNR, the scan resolution would also be effectively increased, since the high-resolution CODEA MRA/MRV at 7T visually demonstrated much enhanced small vessel detectability and reduced susceptibility artifacts, especially for the veins without phase-mask filtering (Fig. 5).

Discussion

Ultra-high-field (UHF) MR imaging, such as 7T imaging, has shown markedly enhanced SNR, blood-to-tissue contrast, and susceptibility effect. This improves the visualization of small arteries and veins in the brain (4,5). We have implemented and tested our newly developed ‘compatible dual-echo arteriovenography (CODEA)’ technique at 7T and compared the image qualities with those acquired at 3T. In our study, the 7T CODEA MRA/MRV showed higher vascular contrast and small-vessel detectability than the 3T CODEA MRA/MRV.

The arterial and venous CNR values for the 7T CODEA MRA/MRV were approximately twice as high as those for the 3T CODEA MRA/MRV. In our study, the relative enhancement of the arterial CNR of the 7T as compared to 3T MRA was 110%, which is

slightly higher yet still comparable to that reported by the other study (83%) (4). The enhanced CNR values at 7T are beneficial for high-resolution imaging as well as increased small-vessel detectability. High-resolution imaging at 7T is also advantageous over normal-resolution imaging for the reduction of susceptibility artifact because of reduced voxel size. While high resolution imaging is desirable at 7T, it also requires a longer scan time. Because of this, CODEA is decidedly useful at 7T because it saves scan time by acquiring both MRA and MRV simultaneously. In our implementation, the scan time for CODEA was exactly the same as that for the individual acquisition of conventional MRA or conventional MRV.

One additional advantage of MRV at 7T is the enhanced venous contrast without phase-mask filtering at the longer TE of 20 ms, which corresponds with the findings reported from a previous study at 9.4T (17). Phase-mask filtering is known to be useful to increase the visibility of the venous vasculature in MRV, particularly at low-fields (18). However, since the venous blood phase is dependent on the vessel orientation and to some degree vessel size, the phase mask processing may not lead to the expected enhancement of the signal in some vessels. Thus, MRV at 7T without phase-mask filtering deems technically more straightforward and reliable than the MRV at 3T.

One drawback of 7T imaging is B_1 field inhomogeneity. The current 8-channel coil used in this study yielded brighter signals around peripheries, while the single-channel circularly-polarized coil used in our previous study gave brighter signals around the center (22). In either case, the B_1 field inhomogeneity at 7T did not cause significant problems in our gradient echo imaging without any specific correction method.

The proposed CODEA technique will likely be useful for both physiological studies and clinical diagnostic applications. For instance, in clinical acute stroke studies TOF MRA has been routinely performed for identification of arterial occlusion and recanalization after treatments. BOLD MR venography is also an important imaging modality for the appropriate assessment of hemorrhagic transformation, blood clots, and venous shape changes after onset of acute stroke. Recently there have been limited trials of BOLD MR venography (MRV) (also known as susceptibility weighted imaging (20)) for acute stroke patients. One of the studies demonstrated detectability of hemorrhage more reliable than the conventional CT method (23). Nevertheless, BOLD MRV is performed infrequently in clinical acute stroke studies, because scan time allowed for acute stroke patients is extremely limited. This scan time constraint may be overcome with CODEA in that we will be able to acquire the potentially valuable BOLD MRV with no additional examination time by simply replacing the conventional single-echo TOF MRA with CODEA. In particular, CODEA at 7T allows us to obtain MRA and MRV with the image quality far better than CODEA at 3T.

In conclusion, compared to 3T, the dual-echo arteriovenography technique we implemented at 7T allows the improved visualization of small vessels in both the MRA and MRV because of the greatly increased SNR and susceptibility contrast.

Acknowledgments

Grant Support : Supported in part by a NIH grant NS064448.

References

1. Chen CN, Sank VJ, Cohen SM, Hoult DI. The field dependence of NMR imaging. I. Laboratory assessment of signal-to-noise ratio and power deposition. Magn Reson Med. 1986; 3(5):722–729. [PubMed: 3784889]
2. Ogawa S, Lee TM. Magnetic resonance imaging of blood vessels at high fields: in vivo and in vitro measurements and image simulation. Magn Reson Med. 1990; 16(1):9–18. [PubMed: 2255240]

3. Ogawa S, Lee TM, Nayak AS, Glynn P. Oxygenation-sensitive contrast in magnetic resonance image of rodent brain at high magnetic fields. Magn Reson Med. 1990; 14(1):68–78. [PubMed: 2161986]
4. von Morze C, Xu D, Purcell DD, et al. Intracranial time-of-flight MR angiography at 7T with comparison to 3T. J Magn Reson Imaging. 2007; 26(4):900–904. [PubMed: 17896360]
5. Deistung A, Rauscher A, Sedlacik J, Stadler J, Witoszynskyj S, Reichenbach JR. Susceptibility weighted imaging at ultra high magnetic field strengths: theoretical considerations and experimental results. Magn Reson Med. 2008; 60(5):1155–1168. [PubMed: 18956467]
6. Wehrli FW, Shimakawa A, Gullberg GT, MacFall JR. Time-of-flight MR flow imaging: selective saturation recovery with gradient refocusing. Radiology. 1986; 160(3):781–785. [PubMed: 3526407]
7. Reichenbach JR, Venkatesan R, Schillinger DJ, Kido DK, Haacke EM. Small vessels in the human brain: MR venography with deoxyhemoglobin as an intrinsic contrast agent. Radiology. 1997; 204(1):272–277. [PubMed: 9205259]
8. Lee BC, Vo KD, Kido DK, et al. MR high-resolution blood oxygenation level-dependent venography of occult (low-flow) vascular lesions. AJNR Am J Neuroradiol. 1999; 20(7):1239–1242. [PubMed: 10472978]
9. Tan IL, van Schijndel RA, Pouwels PJ, et al. MR venography of multiple sclerosis. AJNR Am J Neuroradiol. 2000; 21(6):1039–1042. [PubMed: 10871010]
10. Sehgal V, Delproposto Z, Haacke EM, et al. Clinical applications of neuroimaging with susceptibility-weighted imaging. J Magn Reson Imaging. 2005; 22(4):439–450. [PubMed: 16163700]
11. Du YP, Jin Z. Simultaneous acquisition of MR angiography and venography (MRAV). Magn Reson Med. 2008; 59(5):954–958. [PubMed: 18429022]
12. Deistung A, Dittrich E, Sedlacik J, Rauscher A, Reichenbach JR. ToF-SWI: Simultaneous time of flight and fully flow compensated susceptibility weighted imaging. J Magn Reson Imaging. 2009; 29(6):1478–1484. [PubMed: 19472425]
13. Park SH, Moon CH, Bae KT. Compatible dual-echo arteriovenography (CODEA) using an echo-specific K-space reordering scheme. Magn Reson Med. 2009; 61(4):767–774. [PubMed: 19191284]
14. Parker DL, Yuan C, Blatter DD. MR angiography by multiple thin slab 3D acquisition. Magn Reson Med. 1991; 17(2):434–451. [PubMed: 2062215]
15. Edelman RR, Ahn SS, Chien D, et al. Improved time-of-flight MR angiography of the brain with magnetization transfer contrast. Radiology. 1992; 184(2):395–399. [PubMed: 1620835]
16. Pike GB, Hu BS, Glover GH, Enzmann DR. Magnetization transfer time-of-flight magnetic resonance angiography. Magn Reson Med. 1992; 25(2):372–379. [PubMed: 1614322]
17. Park SH, Masamoto K, Hendrich K, Kanno I, Kim SG. Imaging brain vasculature with BOLD microscopy: MR detection limits determined by in vivo two-photon microscopy. Magn Reson Med. 2008; 59(4):855–865. [PubMed: 18383285]
18. Reichenbach JR, Haacke EM. High-resolution BOLD venographic imaging: a window into brain function. NMR Biomed. 2001; 14(7–8):453–467. [PubMed: 11746938]
19. Blatter DD, Parker DL, Robison RO. Cerebral MR angiography with multiple overlapping thin slab acquisition. Part I. Quantitative analysis of vessel visibility. Radiology. 1991; 179(3):805–811. [PubMed: 2027996]
20. Haacke EM, Xu Y, Cheng YC, Reichenbach JR. Susceptibility weighted imaging (SWI). Magn Reson Med. 2004; 52(3):612–618. [PubMed: 15334582]
21. Koopmans PJ, Manniesing R, Niessen WJ, Viergever MA, Barth M. MR venography of the human brain using susceptibility weighted imaging at very high field strength. Magma. 2008; 21(1–2):149–158. [PubMed: 18188626]
22. Bae KT, Park SH, Moon CH, Kim JH. Compatible dual-echo arteriovenography (CODEA) imaging at 7T versus 3T. Proc Intl Soc Magn Reson Med. 2009:1864.
23. Wycliffe ND, Choe J, Holshouser B, Oyoyo UE, Haacke EM, Kido DK. Reliability in detection of hemorrhage in acute stroke by a new three-dimensional gradient recalled echo susceptibility-

weighted imaging technique compared to computed tomography: a retrospective study. J Magn Reson Imaging. 2004; 20(3):372–377. [PubMed: 15332242]

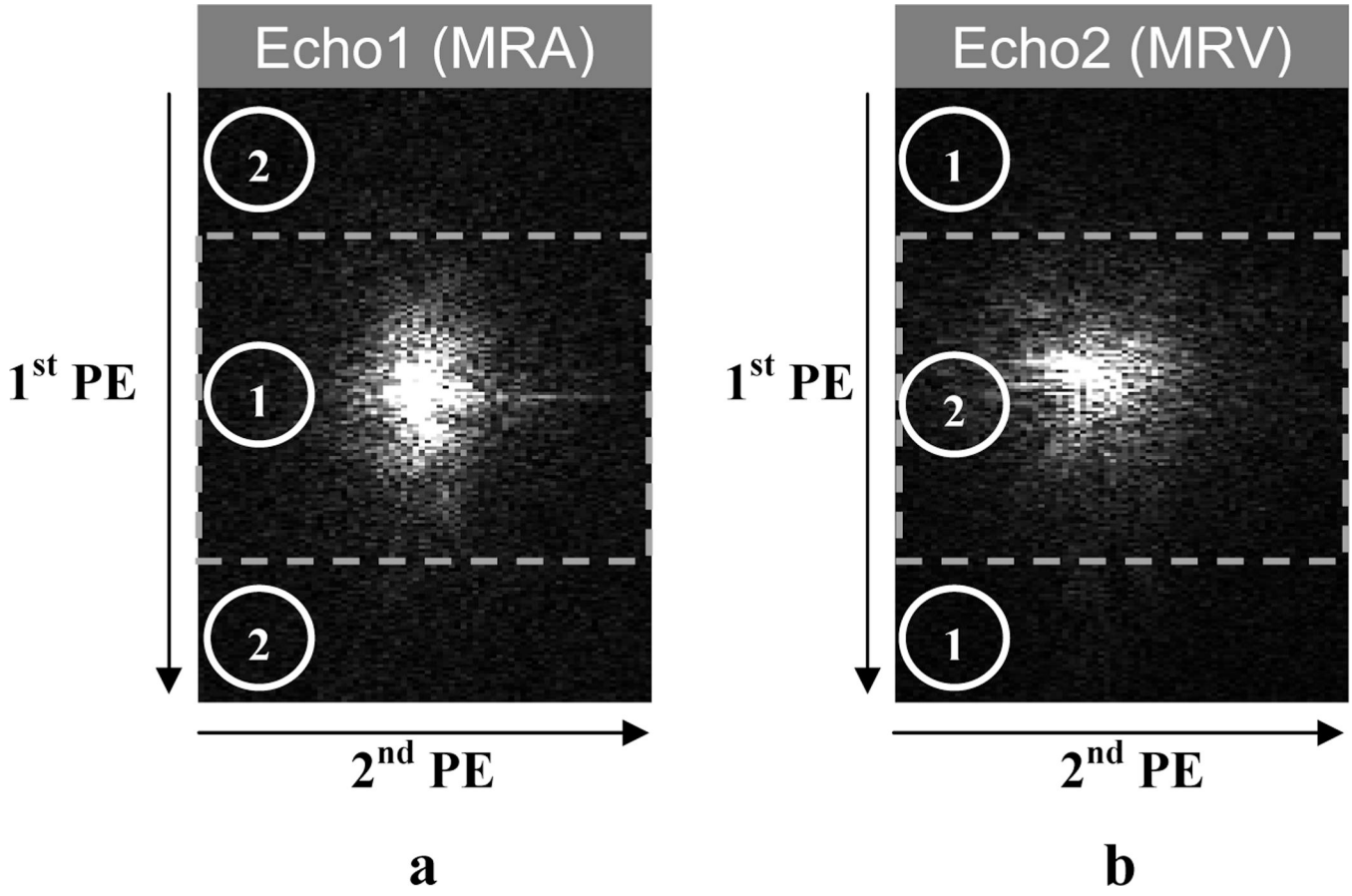

Fig. 1. Echo-specific K-space reordering scheme

The K-space images were from an *in vivo* data reconstructed at the plane of the center of the first echo (**a**) and the second echo (**b**). The 1st PE corresponds to the in-plane phase encoding direction while the 2nd PE to the slice encoding direction. The rectangular line divides the K-space center and edge regions in the K-spaces in each echo. The numbers within the circles represent the data acquisition order in the echo-specific K-space reordering scheme.

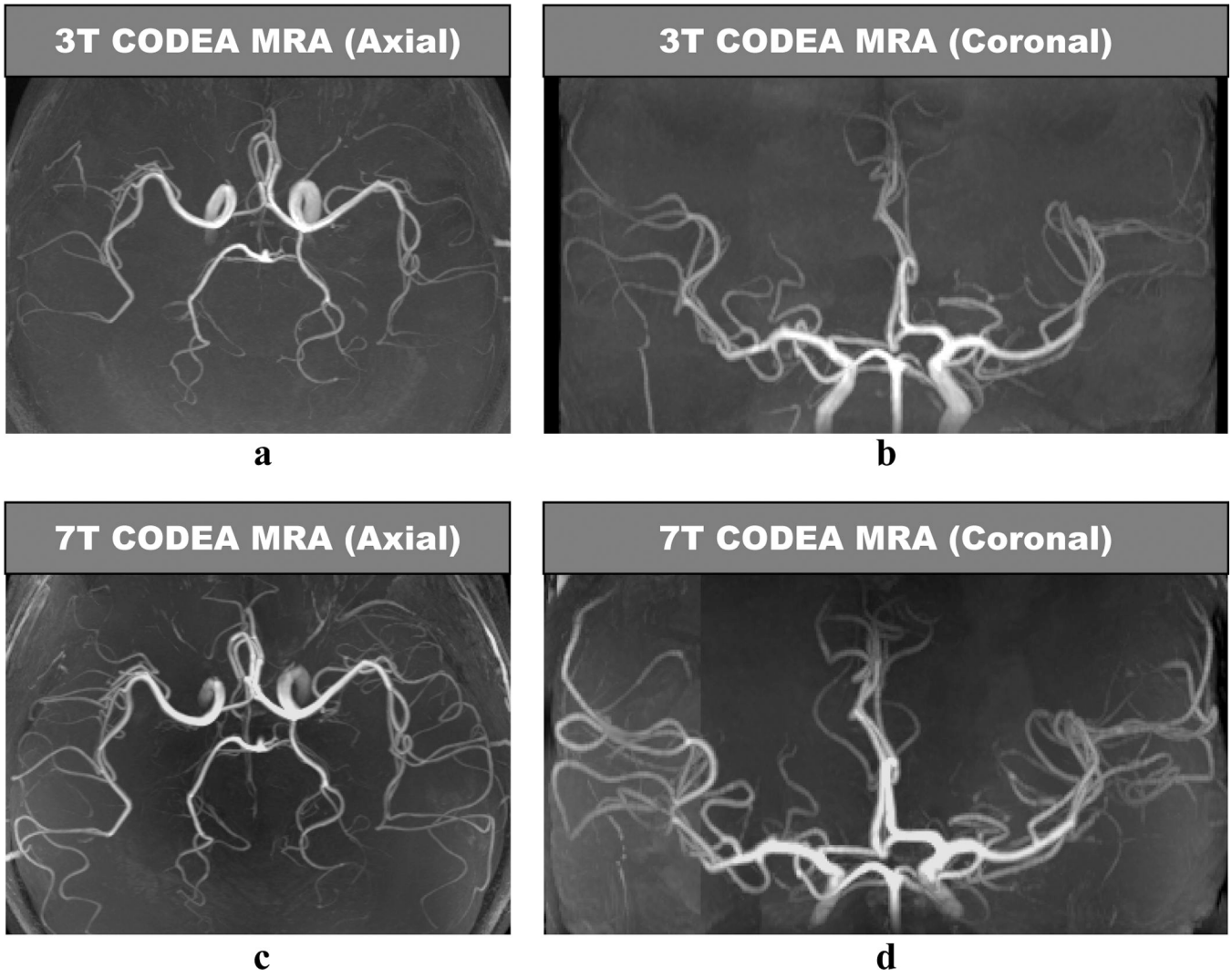

Fig. 2. Comparison of CODEA MRAs acquired at 3T and 7T

The MRA images are represented at maximum intensity projections over the entire volume. The overall arterial contrast and the small vessel detectability of the 7T images (**c** and **d**) are higher than those for the 3T images (**a** and **b**).

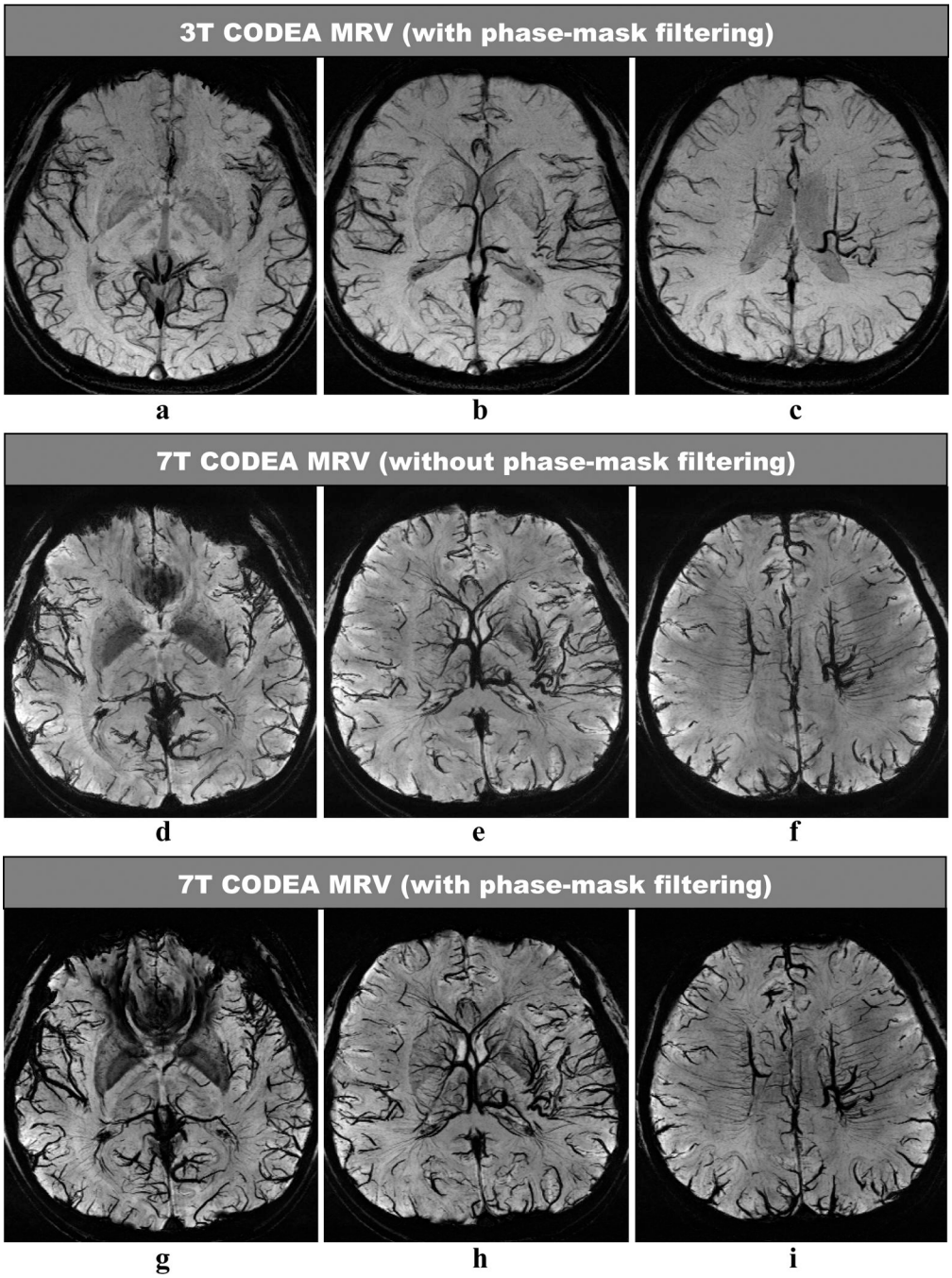

Fig. 3. Comparison of CODEA MRVs acquired at 3T and 7T

The MRV images are represented at minimum intensity projections over 10-mm thickness. The overall venous contrast and the small vessel detectability of the 7T images (**d–i**) are higher than those for the 3T images (**a–c**). Note that the 7T MRV showed improved venous contrast even without phase-mask filtering (**d–f**), compared to the 3T MRV.

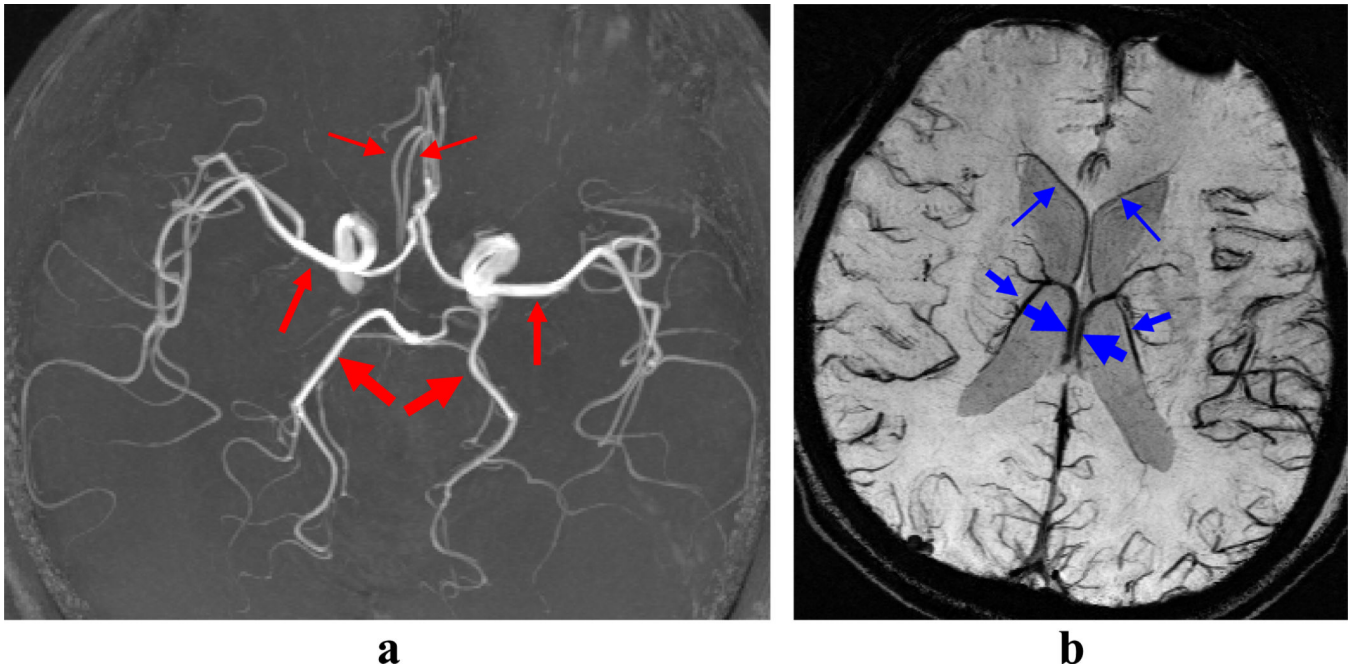

Fig. 4. Blood vessels used for CNR quantifications

Arteries in the MRA images (**a**) and veins in the MRV images (**b**) used in the CNR quantifications are indicated by red and blue arrows, respectively. The thickness of the arrows corresponds to the thickness of blood vessels (“large”, “medium”, and “small”). The images were acquired at 3T from a subject different from those used in Figures 2, 3, and 5. The MRA image (**a**) is a maximum-intensity projection applied to the entire volume and the MRV images (**b**) is a minimum-intensity projection applied over 10 mm thickness with phase-mask filtering.

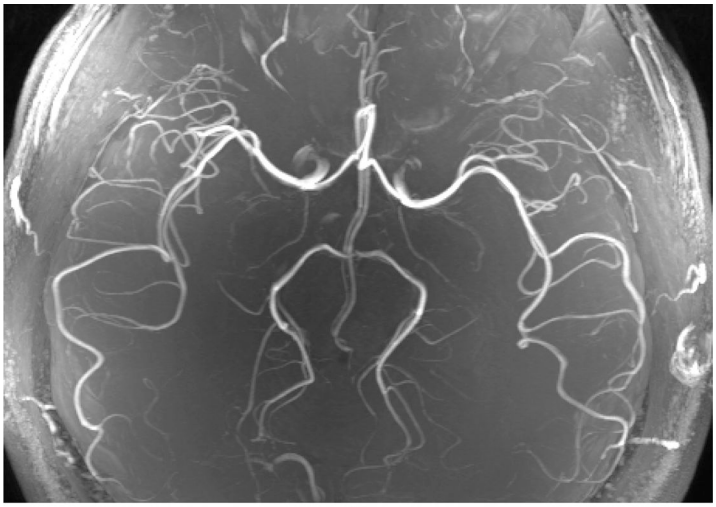

a

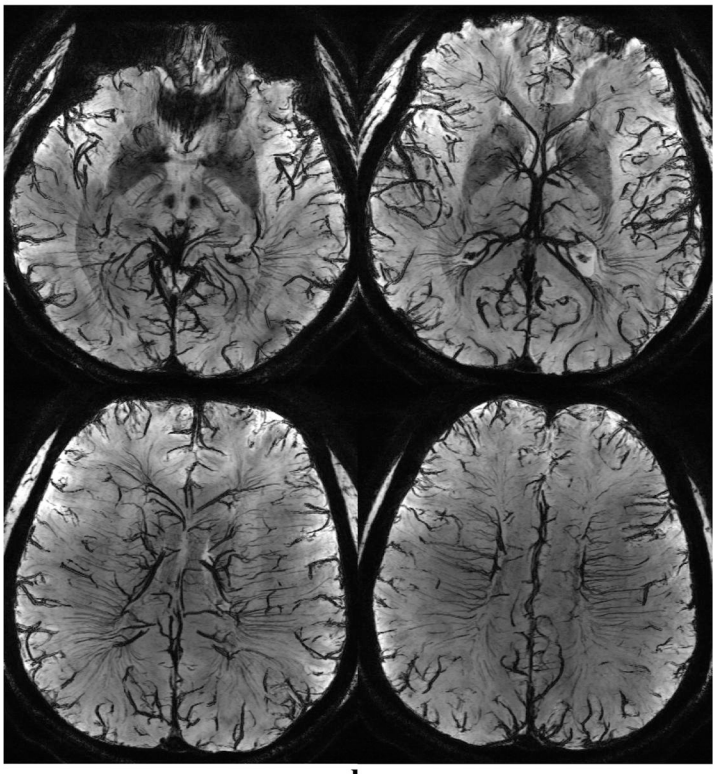

b

Fig. 5. High resolution CODEA images acquired at 7T

The MRA images (**a**) are maximum-intensity projections applied to the entire volume and the MRV images (**b**) are minimum-intensity projections applied over 10 mm thickness without phase-mask filtering.

Table 1

Comparisons of contrast to noise ratio (CNR) for CODEA MRA/MRV acquired at 7T vs 3T

The blood vessels are indicated by arrows in Fig. 4, with the sizes of blood vessels corresponding to the thickness of the arrows. The CNR values are given as mean ± standard deviation. The values within the parentheses in the "CNR at 7T" column indicate those from CODEA MRV without phase-mask filtering.

Blood vessels	CNR at 7T	CNR at 3T	Ratio (7T / 3T)
Artery 1 ("large")	218±55	108±14	2.0
Artery 2 ("medium")	116±10	72±12	1.6
Artery 3 ("small")	159±44	51±8	3.1
Vein 1 ("large")	73±4 (66±5)	42±6	1.7
Vein 2 ("medium")	77±10 (69±8)	36±3	2.1
Vein 3 ("small")	67±5 (61±7)	31±2	2.2